

Dynamics of the measurement uncertainty in an open system and its controlling

Yu-Bing Yao¹, Dong Wang^{1,2} , Fei Ming¹ and Liu Ye¹

¹School of Physics & Material Science, Anhui University, Hefei 230601, People's Republic of China

²CAS Key Laboratory of Quantum Information, University of Science and Technology of China, Hefei 230026, People's Republic of China

E-mail: dwang@ahu.edu.cn

Received 29 June 2019, revised 27 October 2019

Accepted for publication 13 November 2019

Published 6 January 2020



CrossMark

Abstract

The uncertainty principle is one of the most remarkable features of quantum mechanics, originally expressed in terms of the standard deviation of two incompatible observables. Alternatively, it can be modified and written in the form of entropy to eliminate the defect in the form of standard deviation, and can also be generalized by including a memory particle that is entangled with the particle to be measured. Herein we consider a realistic scenario where the particle A to be measured is in an open environment and B as quantum memory is under an environment typically characterized by non-Markovian regimes. Specifically, it shows that the quantum memory and the non-Markovian effect can essentially inhibit the increase of uncertainty, however, the quantum memory-assisted uncertainty will finally inflate inevitably, due to that the quantum correlation of the system will be damaged gradually by the noise from the surrounding environments. To be explicit, we study the dynamic evolution of the entropic uncertainty and correlation in open system where both particles experience the noise channels. Meanwhile, we put forward some effective operation strategies to reduce the magnitude of the measurement uncertainty under the open systems. Furthermore, we explore the applications of the uncertainty relation investigated on entanglement witness and quantum channel capacity. Thus, our investigations might offer an insight into quantum measurement estimation in open systems.

Keywords: entropic uncertainty relation, open system, quantum memory, quantum correlation

(Some figures may appear in colour only in the online journal)

1. Introduction

The uncertainty principle is the pillar in the regime of quantum theory which embodies one of its characteristics: inevitable uncertainty limiting our ability to predict the measurement results of two incompatible observable simultaneously. The Heisenberg's uncertainty principle is one of the most prominent features of quantum theory [1], and it provides a bound on predicting the measurement outcomes of two incompatible observables. After that, Kennard [2, 3] formalized Heisenberg original ideas in an uncertainty relations by a pair of observables: position x and momentum p_x , with the famous inequality [4, 5]

$$\Delta x \Delta p_x \geq \frac{\hbar}{2}, \quad (1)$$

where $\Delta x(\Delta p_x)$ represents the standard deviation of the observable $x(p_x)$. Later, this relation was generalized by Robertson [6] for two arbitrary observables R and S , viz.

$$\Delta R \Delta S \geq \frac{|\langle \psi | [R, S] | \psi \rangle|}{2}. \quad (2)$$

It should be noted that this inequality exhibits a conceptual shortcoming that the right-side (uncertainty bound) of this inequality is state-dependent [7]. As a result, it may become trivial when the commutator $[R, S]$ has zero expectation value in a system with one of the eigenstates related to R or S .

In this regard, Deutsch [8] presented another uncertainty relation via Shannon entropy instead of the standard deviation, which is independent of the system state [9]. Canonically, this new inequality is termed as entropic uncertainty relations (EUR). If we use define the $p(x)$ as the probability of

the outcome x in a given system, the Shannon entropy can be expressed as $H(x) = -\sum_x p(x) \log_2 p(x)$. The EUR for any two general observables was first given by Deutsch and Kraus [8, 10], then proved by Maassen and Uffink [11]. Mathematically, the promising relations for two incompatible Q and R can be described as

$$H(R) + H(Q) \geq \log_2 \frac{1}{c}, \quad (3)$$

where $c = \max_{i,j} |\langle \psi_i | \phi_j \rangle|^2$ and denote the complementarity between Q and R , $|\psi_i\rangle$ and $|\phi_j\rangle$ are the eigenvectors of Q and R . To date, there have been several promising investigations with respect to the entropic uncertainty under the influence of various types of dissipative environments [12–18].

Recently, Berta *et al* [19] have derived a new type of uncertainty relations, which was called as quantum memory-assisted entropic uncertainty relations (QMA-EUR) [20–23], and the equivalent form was originally conjectured by Renes and Boileau [24]. Explicitly, one can illustrate the uncertainty relations by virtue of the following uncertainty game between two participators Alice and Bob. In this game, Alice and Bob beforehand agree on implementing measurement either Q or R . And Bob prepares a qubit A which is entangled with his quantum memory B , and sends it to Alice through quantum channels. Alice then carries out one of the two measurements and tells her choice to Bob. Bob’s task is to minimize his uncertainty about Alice’s measurement outcome. Under such a setting, Berta *et al* reported that a more general uncertainty relations holds [19]

$$S(Q|B) + S(R|B) \geq \log_2 \frac{1}{c} + S(A|B), \quad (4)$$

where $S(A|B) = S(\rho_{AB}) - S(\rho_B)$ [4] is the conditional von Neumann entropy and c is the complementarity between Q and R . While $S(\rho) = -\text{tr}[\rho \log_2 \rho]$ denotes the von Neumann entropy [4, 25]. $S(X|B)$ with $X \in (Q, R)$ represents the conditional entropies of the post-measurement states $\rho_{XB} = \sum_i (|\psi_i\rangle \langle \psi_i| \otimes \mathbb{1}) \rho_{AB} (|\psi_i\rangle \langle \psi_i| \otimes \mathbb{1})$ after the subsystem A is measured in X -basis, $|\psi_i\rangle$ are the eigenstates of the observable X , and $\mathbb{1}$ is the identity matrix. In addition, the QMA-EUR is very useful and has been widely applied to various appealing aspects in the region of quantum information science [26–29], including quantum randomness [30], quantum key distribution [31, 32], cryptography [33, 34], entanglement witnessing [19, 22, 35], quantum metrology [36, 37].

As we know, the quantum objects are inevitably interacting with their surrounding environments [38], which will induce quantum decoherence and dissipation effects. As a result, it is required and of basic importance to make it clear how quantum decoherence and dissipation effects act on the dynamics of QMA-EUR in open systems.

In this article, we investigate the dynamic evolution of the entropic uncertainty in open systems. Specifically, we observe the dynamical evolution of the entropic uncertainty when particle A suffers from generalized amplitude damping (GAD) or depolarization (DP) channel, and quantum memory B from a colored dephasing noise. Generally, a GAD channel

can be modeled by Kraus operators [4]

$$\begin{aligned} \hat{E}_1 &= \sqrt{p} \begin{pmatrix} 1 & 0 \\ 0 & \sqrt{1-r} \end{pmatrix}, \hat{E}_2 = \sqrt{p} \begin{pmatrix} 0 & \sqrt{r} \\ 0 & 0 \end{pmatrix}, \\ \hat{E}_3 &= \sqrt{1-p} \begin{pmatrix} \sqrt{1-r} & 0 \\ 0 & 1 \end{pmatrix}, \hat{E}_4 = \sqrt{1-p} \begin{pmatrix} 0 & 0 \\ \sqrt{r} & 0 \end{pmatrix}, \end{aligned} \quad (5)$$

where p is the probability of the corresponding decay and the decay strength $r = 1 - e^{-\varepsilon t}$, and ε denotes the energy relaxation rate. Additionally, a DP noise can also be described by the following four Kraus operators [4]

$$\begin{aligned} \hat{E}_1 &= \sqrt{1 - \frac{3p}{4}} \begin{pmatrix} 1 & 0 \\ 0 & 1 \end{pmatrix}, \hat{E}_2 = \sqrt{\frac{p}{4}} \begin{pmatrix} 0 & 1 \\ 1 & 0 \end{pmatrix}, \\ \hat{E}_3 &= \sqrt{\frac{p}{4}} \begin{pmatrix} 0 & -i \\ i & 0 \end{pmatrix}, \hat{E}_4 = \sqrt{\frac{p}{4}} \begin{pmatrix} 1 & 0 \\ 0 & -1 \end{pmatrix}, \end{aligned} \quad (6)$$

where p denotes the probability of polarization with $p = 1 - e^{-\gamma t}$, and γ denotes the energy relaxation rate. Herein, we aim to reveal the evolutionary characteristics of measurement’s uncertainty in such scenarios. What’s more, we have put forward two effective operation strategies to govern the magnitude of the measurement uncertainty by means of quantum weak measurement and filtering operation, respectively. Finally, we focus on the applications of the examined uncertainty relation on entanglement witness and quantum channel capacity.

2. The dynamical characteristics of the measurement’s uncertainty under decoherence

2.1. Model

It is well known that any quantum system is non-isolated from its surrounding environment, and thus inevitably coupled with its surrounding noises, which will lead to the decoherence or dissipation effects. In this regard, we here focus on concerning a model that particle A to be measured is in an open environment suffering from GAD or DP decoherence.

On the other hand, particle B as quantum memory is subject to a canonical colored dephasing (CD) noise, which was introduced by Daffer *et al* [39]. As to a colored dephasing noise, the dynamics can be described by a master equation of the form

$$\dot{\rho} = \mathcal{K}(t)\mathcal{L}\rho, \quad (7)$$

where \mathcal{K} acts on the memory particle B as

$$\mathcal{K}(t)\phi = \int_0^t k(t-t')\phi(t')dt', \quad (8)$$

with $k(t-t')$ being a kernel function determining the type of memory in the environment, ρ is the density operator of the particle B , and \mathcal{L} is a Lindblad superoperator. In order to investigate a master equation of this form, one can take into account a time-dependent Hamiltonian $\mathcal{H}(t) = \hbar\Upsilon(t)\sigma_z$, with the Pauli operator σ_z and $\Upsilon(t)$ denoting an independent random variable with the statistics of a random telegraph signal. In particular, the random variable $\Upsilon(t)$ can be expressed as

$\Upsilon(t) = \alpha n(t)$, herein α is a coin-flip random variable with one value of $\pm\alpha$ and $n(t)$ exhibits a Poisson distribution with a mean equaling to $t/2\tau$. Under $\alpha = 1$, the dynamics of the memory particle is able to be depicted by the following Kraus operators [39, 40]

$$\begin{aligned} \hat{K}_1(\nu) &= \sqrt{\frac{1 + \Lambda(\nu)}{2}} \mathbb{1}, \\ \hat{K}_2(\nu) &= \sqrt{\frac{1 - \Lambda(\nu)}{2}} \sigma_z, \end{aligned} \quad (9)$$

within the above, $\Lambda(\nu) = e^{-\nu} [\cos(\mu\nu) + \frac{\sin(\mu\nu)}{\mu}]$ with $\nu = t/2\tau$ being the scaled time, and $\mu = \sqrt{(4\tau)^2 - 1}$. The parameter τ controls the degree of non-Markovianity producing the memory effects. As a result, this noise is characterized by being non-Markovian.

Therefore, after the state passing through the noises, the evolution density matrix can be written in sum-operator representation as

$$\rho_{AB}(t) = \sum_{i=1, j=1}^{i=4, j=2} (\hat{E}_i \otimes \hat{K}_j) \rho_{AB}(0) (\hat{E}_i \otimes \hat{K}_j)^\dagger, \quad (10)$$

where, $\rho_{AB}(0)$ represents an initial state of the composite system, and $\rho_{AB}(t)$ denotes the systemic final state.

In what follows, we will elaborate the dynamics of entropic uncertainty in the situation where the particle A suffers from the GAD or DP noise and the particle B is subject to the non-Markovian noise (CD).

2.2. GAD+CD noises

To probe the dynamic of the QMA-EUR, we can resort to Pauli operators σ_x and σ_z as the incompatible observables. As a consequence, the entropy-based uncertainty and the lower bound in equation (4) can be expressed by

$$U = S(\sigma_x|B) + S(\sigma_z|B), \quad (11)$$

$$U_b = \log_2 \frac{1}{c} + S(A|B) \quad (12)$$

respectively. Since σ_x and σ_z are mutual unbiased basis, $\frac{1}{c}$ remains the value 2 in a qubit system, which implies that $\log_2 \frac{1}{c} = 1$. On the other hand, with respect to a bipartite system, its quantum correlation can be quantified by the so-called quantum discord (QD), which has intrinsic hierarchical relation with the other resources including concurrence [41], Bell non-locality [42, 43] and quantum steering [44–46], and remarkably it is regarded a a more general resource than those mentioned. Basically, QD can be written as [47–49]

$$Q(\rho_{AB}) = I(\rho_{AB}) - C(\rho_{AB}) = \min\{Q_1, Q_2\}, \quad (13)$$

where $C(\rho_{AB}) = S(\rho_A) - \min_{\Pi_i^B} S_{\Pi_i^B}(\rho_{A|B})$ denotes the classical correlation and Π_i^B denotes a sets of possible positive-operator-valued measurement on particle B , $S_{\Pi_i^B}(\rho_{A|B}) = \sum_i q_i S(\rho_i^A)$ is the conditional entropy of particle A , $\rho_i^A = Tr_B(\Pi_i^B \rho_{AB} \Pi_i^B) / q_i$ denotes the density matrix with the corresponding probability $q_i = Tr_{AB}(\rho_{AB} \Pi_i^B)$, $I(\rho_{AB}) =$

$S(\rho_A) + S(\rho_B) - S(\rho_{AB})$ represents the mutual information between A and B . In addition, we have

$$Q_j = H_{bin}(\rho_{11} + \rho_{33}) + \sum_{i=1}^4 \lambda_i^{AB} \log_2 \lambda_i^{AB} + D_j \quad (14)$$

with

$$\begin{aligned} D_1 &= H_{bin}(\delta), \\ D_2 &= -\sum_i \rho_{ii} \log_2 \rho_{ii} - H_{bin}(\rho_{11} + \rho_{33}), \end{aligned} \quad (15)$$

with $\delta = \{1 + \sqrt{[1 - 2(\rho_{44} + \rho_{33})]^2 + 4(|\rho_{14}| + |\rho_{23}|)}\} / 2$, and $H_{bin}(x) = -x \log_2 x - (1 - x) \log_2 (1 - x)$ represent a binary entropy.

In the current scenario, we consider the initial of the bipartite system AB with the form of Bell-diagonal state (BDS)

$$\rho_{AB}(0) = \frac{1}{4} (\mathbb{1}^A \otimes \mathbb{1}^B + \sum_{j=1}^3 C_j \sigma_j^A \otimes \sigma_j^B), \quad (16)$$

where σ_j with $j \in \{1, 2, 3\}$ are the standard Pauli matrices, and the coefficients $C_j = tr_{AB}(\rho_{AB} \sigma_j^A \otimes \sigma_j^B)$ satisfy $0 \leq |C_j| \leq 1$. As to BDS, they contain the abundant ensembles of both pure and mixed states, which is popular in the current experiments [50–53].

After experiencing the noisy channels, the density matrix of the systemic state $\rho_{AB}(t)$ for AB is with the elements

$$\begin{aligned} \rho_{11} &= \frac{1}{4} (1 + C_3 - (1 + C_3 - 2p)r), \\ \rho_{22} &= \frac{1}{4} (1 - C_3 + (-1 + C_3 + 2p)r), \\ \rho_{33} &= \frac{1}{4} (1 + C_3(-1 + r) + r - 2pr), \\ \rho_{44} &= \frac{1}{4} (1 + C_3 + r - (C_3 + 2p)r), \\ \rho_{23} &= \rho_{32} = (C_1 + C_2)\Omega, \\ \rho_{14} &= \rho_{41} = (C_1 - C_2)\Omega, \end{aligned} \quad (17)$$

according to equations (10) and (16), where

$$\begin{aligned} \Omega &= e^{-t/2\tau} \sqrt{1-r} (\sqrt{16\tau^2 - 1} \cos(\sqrt{16\tau^2 - 1} t/2\tau) \\ &\quad + \sin(\sqrt{16\tau^2 - 1} t/2\tau) / [4\sqrt{16\tau^2 - 1}]). \end{aligned}$$

Since the post-measurement state can be given by

$$\begin{aligned} \rho_{\sigma_x B} &= \frac{1}{4} (|00\rangle\langle 00| + |01\rangle\langle 01| + |10\rangle\langle 10| + |11\rangle\langle 11|) \\ &\quad + C_1 \Omega (|00\rangle\langle 11| + |01\rangle\langle 10| \\ &\quad + |10\rangle\langle 01| + |11\rangle\langle 00|), \\ \rho_{\sigma_z B} &= \sum_{i,j=0,1} \lambda_{ij}^{\sigma_z B} |ij\rangle\langle ij|, \end{aligned} \quad (18)$$

and the von Neumann entropies to quantify the uncertainty of the measurement outcomes for the observables can be

given by

$$\begin{aligned} S(\rho_{\sigma_x B}) &= H_{bin}\left(\frac{1 - 4C_1\Omega}{2}\right) + 1, \\ S(\rho_{\sigma_z B}) &= - \sum_{i,j=0,1} \lambda_{ij}^{\sigma_x B} \log_2 \lambda_{ij}^{\sigma_x B}. \end{aligned} \quad (19)$$

with the eigenvalues of $\rho_{\sigma_z B}$

$$\begin{aligned} \lambda_{00}^{\sigma_z B} &= \frac{1 + C_3 - (1 + C_3 - 2p)r}{4}, \\ \lambda_{01}^{\sigma_z B} &= \frac{1 - C_3 + (-1 + C_3 + 2p)r}{4}, \\ \lambda_{10}^{\sigma_z B} &= \frac{1 + C_3(-1 + r) + r - 2pr}{4}, \\ \lambda_{11}^{\sigma_z B} &= \frac{1 + C_3 + r - (C_3 + 2p)r}{4}. \end{aligned} \quad (20)$$

On the other hand, the reduced density matrix of the Bell-diagonal state is the maximally mixed state $1/2$, and CD will not change the state of subsystem B . With these in mind, we have two eigenvalues of ρ_B both are $1/2$ and $S(\rho_B) = 1$. Analytically, the measurement uncertainty is equal to

$$U = H_{bin}\left(\frac{1 - 4C_1\Omega}{2}\right) - \sum_{i,j=0,1} \lambda_{ij}^{\sigma_x B} \log_2 \lambda_{ij}^{\sigma_x B} - 1, \quad (21)$$

and the complementarity c of the observables σ_x and σ_z is always $1/2$. Thus, the lower bound U_b of the uncertainty is given by

$$U_b = S(\rho_{AB}) = - \sum_{i=1}^4 \lambda_i^{AB} \log_2 \lambda_i^{AB}, \quad (22)$$

where the λ_i^{AB} are the eigenvalue of $\rho_{AB}(t)$ in forms of

$$\begin{aligned} \lambda_1^{AB} &= \frac{1}{4}(1 + C_3 - C_3r - \sqrt{\Gamma}), \\ \lambda_2^{AB} &= \frac{1}{4}(1 + C_3 - C_3r + \sqrt{\Gamma}), \\ \lambda_3^{AB} &= \frac{1}{4}(1 - C_3 + C_3r - \sqrt{\Gamma}), \\ \lambda_4^{AB} &= \frac{1}{4}(1 - C_3 + C_3r + \sqrt{\Gamma}), \end{aligned} \quad (23)$$

with $\Gamma = r^2 - 4pr^2 + 4p^2r^2 + 16(C_1 - C_2)^2\Omega^2$.

Up to now, we have derived the analytical outcomes of the uncertainty and its bound under the current architecture. Apparently, the result is general in the case of that both A and B experience the noisy channels. In order to better understand the impact of the noise channels for the uncertainty, we would like to wonder how the uncertainty of the system evolve over time when these two channels act on the measured system, separately. In this regard, we will take into account two alternative cases that either A or B solely suffers from the noise.

In order to analyse the dynamics of the EUR in the cases mentioned above, we plot the diagram of the uncertainty U , the bound U_b and the systemic quantum correlation QD as a function of evolving time t in figure 1. Following the figure, the subgraphs (a) and (b) demonstrate the case where B

suffers from the CD noise while A is free from any noise; the subgraphs (c) and (d) depict the case where A suffers from the GAD noise while B is free from any noise; the subgraphs (e) and (f) illustrate the case where A and B are subject to the noises. Explicitly, we randomly set $C_1 = -0.3$, $C_2 = 0.2$, $C_3 = 0.8$.

In the open system, due to the existence of the environmental noises, the information of the system will outflow, which results in the decoherence and dissipation effect and the increase of entropic uncertainty, but the non-Markovian channel will not only cause the outflow of information, but also cause the backflow of information. Moreover, the two processes of outflow and backflow are alternated for the CD noise, and the GAD and DP are both typical Markovian noises that only lead to the outflow of information. In principle, the outflow of information will induce the degradation of the systemic QD and meanwhile the increase of the uncertainty, vice versus. Therefore, one can obtain the distinct oscillations for the uncertainty and QD, as shown in figure 1.

In graphs (a) and (b), the uncertainty oscillates with time, which reflects that the non-Markovian effect is able to inhibit the increase of the uncertainty and its bound. To be explicit, the period can be given by $\frac{2\pi\tau}{\sqrt{(4\tau)^2 - 1}}$, and its quantity will saturate into a fixed value $\pi/2$ for the large τ . And the amplitude of the oscillation becomes smaller and smaller, and eventually the amount of the uncertainty tends to a stable value in the long-time limit. Interestingly, the QD also oscillates with time, and tends to 0. By comparing the uncertainty and QD, it shows that the uncertainty is nearly oppositely-correlated with QD. In subgraphs (c) and (d), the uncertainty increases monotonically with time and tends to a fixed value, while the QD decreases monotonically and vanishes finally. In subgraphs (e) and (f), the uncertainty oscillates and increases monotonically with time, and also saturates to a fixed value, the QD oscillates with time and rapidly tends to 0. By comparison with the first case, the collective effect of GAD and CD noises leads to the stronger monotonicity of the uncertainty in the course of the dynamical process.

2.3. DP+CD noises

To further explore the evolution of measurement uncertainty in open systems, we consider that particle A experiences DP noise, while quantum memory B is the colored dephasing noise characterized by Kraus operators $\hat{K}_1(\nu)$ and $\hat{K}_2(\nu)$. Therefore, after passing through the noise channels, the matrix elements of the systemic state $\rho_{AB}(t)$ will be taken as

$$\begin{aligned} \rho_{11} = \rho_{44} &= \frac{1}{4}(1 + C_3 - C_3p), \\ \rho_{22} = \rho_{33} &= \frac{1}{4}(1 + C_3(p - 1)), \\ \rho_{23} = \rho_{32} &= -(C_1 + C_2)\Delta, \\ \rho_{14} = \rho_{41} &= -(C_1 - C_2)\Delta, \end{aligned} \quad (24)$$

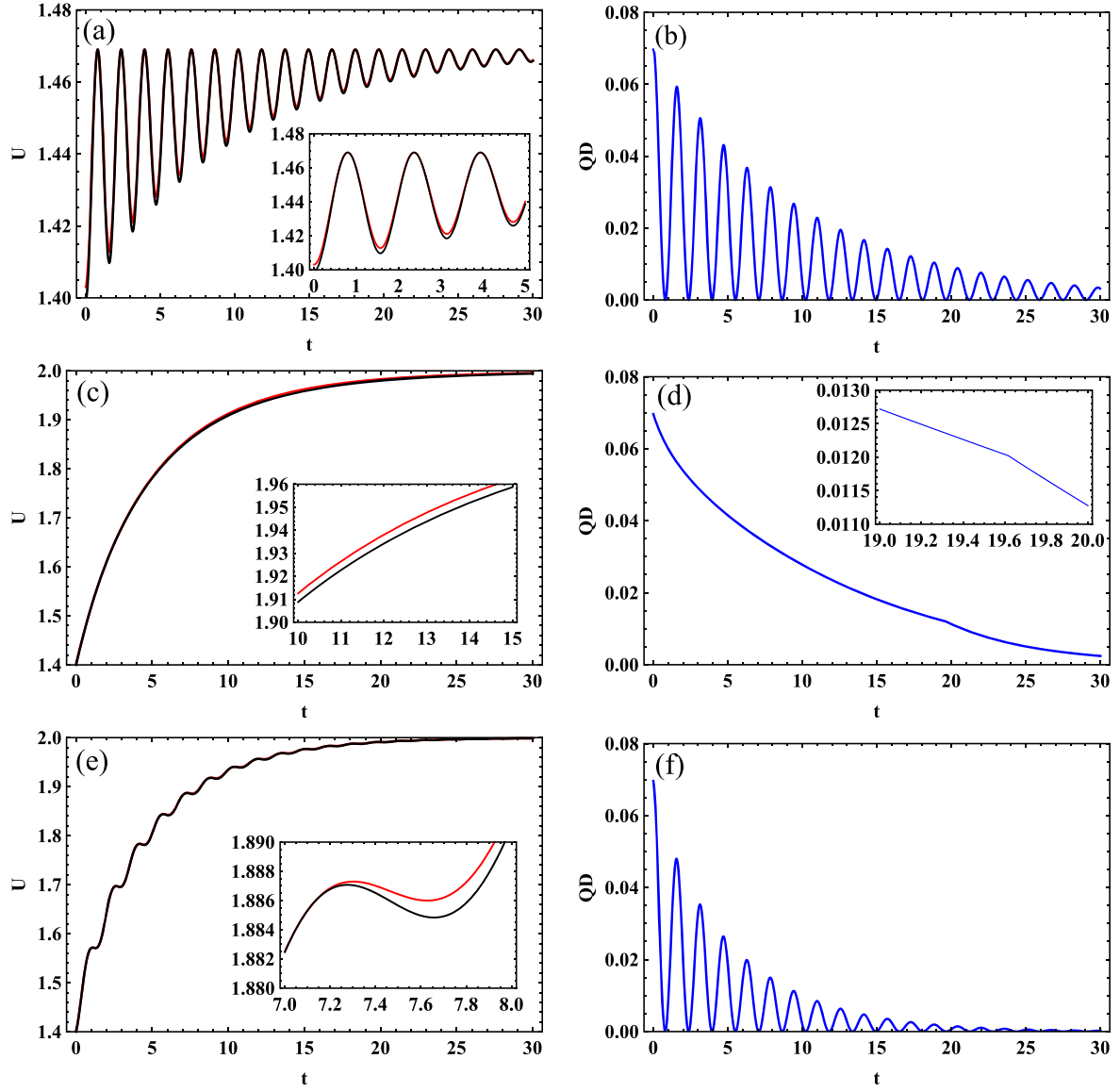


Figure 1. Evolution of entropic uncertainty U (red lines), lower bound U_b (black lines) and QD (blue lines) respected to t when the particle A is under GAD channel. In graphs (a) and (b), we have $\tau = 10$. In graphs (c) and (d), we have $p = 0.5$, $\varepsilon = 0.1$. In graphs (e) and (f), we have $p = 0.5$, $\varepsilon = 0.1$ and $\tau = 10$. $C_1 = -0.3$, $C_2 = 0.2$, $C_3 = 0.8$ are set.

with $\Delta = \frac{e^{-\frac{t}{2\tau}(p-1)} \left(\sqrt{16\tau^2-1} \cos\left(\frac{\sqrt{16\tau^2-1}t}{2\tau}\right) + \sin\left(\frac{\sqrt{16\tau^2-1}t}{2\tau}\right) \right)}{4\sqrt{16\tau^2-1}}$, and the four eigenvalues of $\rho_{AB}(t)$ are

$$\begin{aligned} \tilde{\lambda}_1^{AB} &= \frac{1}{4}(1 + C_3 - C_3p + 4(C_1 - C_2)\Delta), \\ \tilde{\lambda}_2^{AB} &= \frac{1}{4}(1 + C_3 - C_3p - 4(C_1 - C_2)\Delta), \\ \tilde{\lambda}_3^{AB} &= \frac{1}{4}(1 + C_3(p-1) + 4(C_1 + C_2)\Delta), \\ \tilde{\lambda}_4^{AB} &= \frac{1}{4}(1 + C_3(p-1) - 4(C_1 + C_2)\Delta). \end{aligned} \quad (25)$$

After performing measurement σ_x or σ_z on particle A , the post-measurement state can be given by

$$\begin{aligned} \rho_{\sigma_x B} &= \frac{1}{4}(|00\rangle\langle 00| + |01\rangle\langle 01| + |10\rangle\langle 10| + |11\rangle\langle 11|) \\ &\quad - C_1\Delta(|00\rangle\langle 11| + |01\rangle\langle 10| \\ &\quad + |10\rangle\langle 01| + |11\rangle\langle 00|), \\ \rho_{\sigma_z B} &= - \sum_{i,j=0,1} \tilde{\lambda}_{ij}^{\sigma_z B} |ij\rangle\langle ij|, \end{aligned} \quad (26)$$

with

$$\begin{aligned} \tilde{\lambda}_{00}^{\sigma_z B} &= \tilde{\lambda}_{01}^{\sigma_z B} = \frac{1 + C_3 - C_3p}{4}, \\ \tilde{\lambda}_{10}^{\sigma_z B} &= \tilde{\lambda}_{11}^{\sigma_z B} = \frac{1 + C_3(p-1)}{4}, \end{aligned} \quad (27)$$

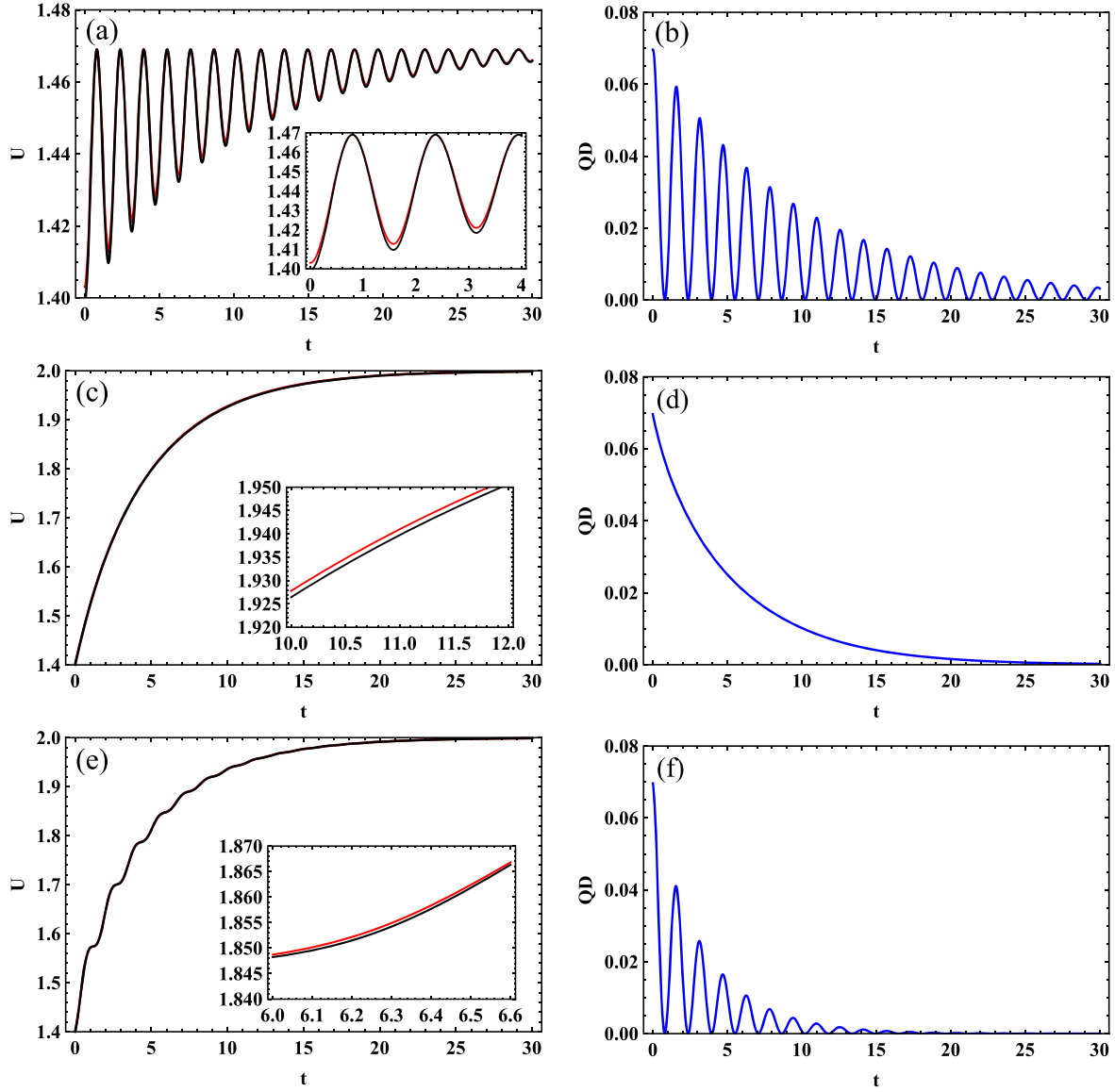


Figure 2. Evolution of entropic uncertainty U (red lines), lower bound U_b (black lines) and QD (blue lines) respected to the t when the particle A is under DP channel. In graphs (a) and (b), we have $\tau = 10$. In graphs (c) and (d), we have $\gamma = 0.1$. In graphs (e) and (f), we have $\tau = 10$ and $\gamma = 0.1$. $C_1 = -0.3$, $C_2 = 0.2$, $C_3 = 0.8$ are set.

their eigenvalues can be obtained easily and lead to the von Neumann entropy

$$S(\rho_{\sigma_x B}) = H_{bin}\left(\frac{1 - 4C_1\Delta}{2}\right) + 1,$$

$$S(\rho_{\sigma_z B}) = H_{bin}\left(\frac{1 + C_3 - C_3p}{2}\right) + 1, \quad (28)$$

and the reduced density matrix ρ_B is still $\mathbb{1}/2$, so the uncertainty can be given by $U = H_{bin}\left(\frac{1 - 4C_1\Delta}{2}\right) + H_{bin}\left(\frac{1 + C_3 - C_3p}{2}\right)$ and its lower bound is $U_b = -\sum_{i=1}^4 \tilde{\lambda}_i^{AB} \log_2 \tilde{\lambda}_i^{AB}$.

Next, let's proceed by revealing the dynamics of entropic uncertainty when the particle A is under DP channel. We plot the uncertainty and lower bound as a function of t in figure 2.

We set $C_1 = -0.3$, $C_2 = 0.2$, $C_3 = 0.8$. In the figure, the graphs corresponding three cases being similar with the scenario mentioned above, In different cases, the dynamic evolution of entropic uncertainty and QD is also different, and has the similar variation tendency with the case in the GAD +CD channels, because GAD and DP both belong to Markovian noises which cause the monotonic increase of uncertainty. Notably, it has been found that the effect of DP to affect the uncertainty seems to be stronger than GAD. In all cases, the lower bound have the same tendency with the uncertainty, and the uncertainty and lower bound are getting closer and closer with the time growth. It needs to note the QMA-EUR holds in all the cases, and the uncertainty is nearly anti-correlated with the QD in the scenario, which is in agreement with the statement made beforehand.

3. Steering

In this section, we would like to develop several effective strategies to steer the uncertainty of the qubit system experiencing the noisy channels through local quantum operations. Actually, a quantum system inevitably interacts with its surrounding noises, which can result in the effect of quantum decoherence. Therefore, how to inhibit the decoherence effect is highly significant in the region of realistic quantum information processing and communication. In recent years, some authors have put forward some promising methods against decoherence, such as quantum weak measurement (QWM) and filtering operation (FO). We are curious about that whether such operations are valid to steer the quantity of the uncertainty. After our investigation, we find the answer is positive. In the followings, we illustrate how these two methods achieve the reduction of the magnitude of the entropic uncertainty.

The quantum weak measurement is a non-trace-preserving map (NTPM) operation, which can be expressed by [54–56]

$$\hat{M} = \begin{pmatrix} 1 & 0 \\ 0 & \sqrt{1-s} \end{pmatrix}, \quad (29)$$

where s denotes the strength of the weak measurement operation and satisfies $0 \leq s \leq 1$. When this operation is performed on qubit A , the final state of the system can read as

$$\rho_{AB}^M(t) = \frac{(\hat{M}^A \otimes \mathbb{1}^B)\rho_{AB}(t)(\hat{M}^A \otimes \mathbb{1}^B)^\dagger}{\text{Tr}\{(\hat{M}^A \otimes \mathbb{1}^B)\rho_{AB}(t)(\hat{M}^A \otimes \mathbb{1}^B)^\dagger\}}. \quad (30)$$

Next, we consider this case where A experiencing DP channels. After the operation acts on A to be observed, the post-operation density matrix of becomes

$$\begin{aligned} \rho_{AB}^M(t) = & \frac{(1 + C_3 - C_3p)}{4(1 - \frac{s}{2})} |00\rangle\langle 00| \\ & + \frac{(1 + C_3(p-1))}{4(1 - \frac{s}{2})} |01\rangle\langle 01| \\ & - \frac{(1 + C_3(p-1))(s-1)}{4(1 - \frac{s}{2})} |10\rangle\langle 10| \\ & + \frac{(-1 + C_3(p-1))(s-1)}{4(1 - \frac{s}{2})} |11\rangle\langle 11| \\ & - \frac{(C_1 - C_2)\Delta\sqrt{1-s}}{1 - \frac{s}{2}} (|00\rangle\langle 11| + |11\rangle\langle 00|) \\ & - \frac{(C_1 + C_2)\Delta\sqrt{1-s}}{1 - \frac{s}{2}} (|01\rangle\langle 10| + |10\rangle\langle 01|). \end{aligned} \quad (31)$$

After A going through the noisy channel, we can obtain the post-measurement state as

$$\begin{aligned} \rho_{\sigma_x B}^M = & \frac{-2 + (1 + C_3(p-1))s}{4(-2 + s)} (|00\rangle\langle 00| + |10\rangle\langle 10|) \\ & + \frac{-2 + (1 + C_3 - C_3p)s}{4(-2 + s)} (|01\rangle\langle 01| + |11\rangle\langle 11|) \\ & + \frac{2C_1\Delta\sqrt{1-s}}{s-2} (|00\rangle\langle 11| + |11\rangle\langle 00| \\ & + |01\rangle\langle 10| + |10\rangle\langle 01|), \\ \rho_{\sigma_z B}^M = & \sum_{i,j=0,1} \lambda_{\sigma_z B ij}^M |ij\rangle\langle ij|. \end{aligned} \quad (32)$$

By calculating their eigenvalues, we can attain the corresponding von Neumann entropies as

$$\begin{aligned} H(\rho_{\sigma_x B}^M) = & H_{bin}\left(\frac{1}{2} - \frac{1}{2(s-2)}\sqrt{\frac{\eta}{16\tau^2 - 1}}\right) + 1, \\ H(\rho_{\sigma_z B}^M) = & - \sum_{i,j=0,1} \lambda_{\sigma_z B ij}^M \log_2 \lambda_{\sigma_z B ij}^M, \end{aligned} \quad (33)$$

with

$$\begin{aligned} \lambda_{\sigma_z B 00}^{\text{DP}} = & \frac{1 + C_3 - C_3p}{4 - 2s}, \\ \lambda_{\sigma_z B 01}^{\text{DP}} = & \frac{1 + C_3(p-1)}{4 - 2s}, \\ \lambda_{\sigma_z B 10}^{\text{DP}} = & \frac{(1 + C_3(p-1))(s-1)}{2(s-2)}, \\ \lambda_{\sigma_z B 11}^{\text{DP}} = & - \frac{(-1 + C_3(p-1))(s-1)}{2(s-2)}, \end{aligned} \quad (34)$$

and

$$\begin{aligned} \eta = & e^{-\frac{t}{\tau}}(p-1)^2(-32C_1^2\tau^2(s-1) + C_3^2(16\tau^2 - 1)e^{\frac{t}{\tau}}s^2 \\ & - 4C_1^2(s-1)\left(-1 + 8\tau^2\right)\cos\left[\frac{\sqrt{16\tau^2 - 1}t}{\tau}\right] \\ & + \sqrt{16\tau^2 - 1}\sin\left[\frac{\sqrt{16\tau^2 - 1}t}{\tau}\right]). \end{aligned}$$

In addition, we have

$$H(\rho_B^M) = - \sum_{k=1}^2 \lambda_{Bk}^M \log_2 \lambda_{Bk}^M, \quad (35)$$

where $\lambda_{B1}^M = \frac{-2 + (1 + C_3(p-1))s}{2(s-2)}$, $\lambda_{B2}^M = \frac{-2 + (1 + C_3 - C_3p)s}{2(s-2)}$. As a result, we can get the entropy-based uncertainty is

$$\begin{aligned} U^M = & H_{bin}\left(\frac{1}{2} - \frac{1}{2(s-2)}\sqrt{\frac{\eta}{16\tau^2 - 1}}\right) \\ & - \sum_{i,j=0,1} \lambda_{\sigma_z B ij}^M \log_2 \lambda_{\sigma_z B ij}^M + 2 \sum_{k=1}^2 \lambda_{Bk}^M \log_2 \lambda_{Bk}^M + 1. \end{aligned} \quad (36)$$

Moreover, the eigenvalues of the state $\rho_{AB}^M(t)$ in equation (31) can be given by

$$\begin{aligned}\lambda_{AB1}^M &= \frac{-2 - 2C_3 + 2C_3p + s + C_3s - C_3ps - \sqrt{\xi}}{4(s-2)}, \\ \lambda_{AB2}^M &= \frac{-2 - 2C_3 + 2C_3p + s + C_3s - C_3ps + \sqrt{\xi}}{4(s-2)}, \\ \lambda_{AB3}^M &= \frac{-2 + 2C_3 + 2C_3p + s + C_3s - C_3ps - \sqrt{\xi}}{4(s-2)}, \\ \lambda_{AB4}^M &= \frac{-2 + 2C_3 + 2C_3p + s + C_3s - C_3ps + \sqrt{\xi}}{4(s-2)},\end{aligned}\quad (37)$$

with $\xi = 64a^2 - 64a^2s + s^2 + 2C_3s^2 + C_3^2s^2 - 2C_3ps^2 - 2C_3^2ps^2 + C_3^2p^2s^2$. And the bound of equation (4) is expressed as

$$U_b^M = -\sum_{j=1}^4 \lambda_{ABj}^M \log_2 \lambda_{ABj}^M - H_{bin}(\lambda_{B1}^M) + 1. \quad (38)$$

In addition, we can utilize the filtering operation to reduce the amount of the measuring uncertainty. The filtering operation is characterized by a non-trace-preserving map (NTPM), which is viewed to be capable of revealing hidden non-locality for some classes of states, and it can recover and increase entanglement to some degree [57, 58]. Practically, this map can be said to be null-result weak measurement [59]. With regard to this operation, it can be written in a computational basis $\{|0\rangle, |1\rangle\}$ as [60, 61]

$$\hat{F} = \begin{pmatrix} \sqrt{1-k} & 0 \\ 0 & \sqrt{k} \end{pmatrix}, \quad (39)$$

where k is the strength of the filtering operation with $0 \leq k \leq 0.5$, after this operation acts on A to be observed, the final state of the system can be written as

$$\rho_{AB}^F(t) = \frac{(\hat{F}^A \otimes \mathbb{1}^B) \rho_{AB}(t) (\hat{F}^A \otimes \mathbb{1}^B)^\dagger}{Tr\{(\hat{F}^A \otimes \mathbb{1}^B) \rho_{AB}(t) (\hat{F}^A \otimes \mathbb{1}^B)^\dagger\}}. \quad (40)$$

After A going through the DP noisy channel, the post-operation state becomes

$$\begin{aligned}\rho_{AB}^F(t) &= \frac{1}{2}(k-1)(-1 + C_3(p-1))|00\rangle\langle 00| \\ &\quad - \frac{1}{2}(k-1)(1 + C_3(p-1))|01\rangle\langle 01| \\ &\quad + \frac{1}{2}k(1 + C_3(p-1))|10\rangle\langle 10| \\ &\quad + \frac{1}{2}k(1 + C_3 - C_3p)|11\rangle\langle 11| \\ &\quad - 2(C_1 - C_2)\Delta\sqrt{(1-k)k}(|00\rangle\langle 11| + |11\rangle\langle 00|) \\ &\quad - 2(C_1 + C_2)\Delta\sqrt{(1-k)k}(|01\rangle\langle 10| + |10\rangle\langle 01|),\end{aligned}\quad (41)$$

and the post-measurement state can be calculated as

$$\begin{aligned}\rho_{\sigma_x B}^F &= \frac{1}{4}(1 + C_3(2k-1)(p-1))(|00\rangle\langle 00| + |10\rangle\langle 10|) \\ &\quad + \frac{1}{4}(1 + C_3(-1 - 2k(p-1) + p))(|01\rangle\langle 01| \\ &\quad + |11\rangle\langle 11|) - 2C_1\Delta\sqrt{(1-k)k}(|00\rangle\langle 11| + |11\rangle\langle 00| \\ &\quad + |01\rangle\langle 10| + |10\rangle\langle 01|), \\ \rho_{\sigma_z B}^F &= \sum_{i,j=0,1} \lambda_{\sigma_z Bij}^F |ij\rangle\langle ij|,\end{aligned}\quad (42)$$

leading to the von Neumann entropy

$$\begin{aligned}H(\rho_{\sigma_x B}^F) &= H_{bin}\left(\frac{1 + \sqrt{\zeta}}{2}\right) + 1, \\ H(\rho_{\sigma_z B}^F) &= -\sum_{i,j=0,1} \lambda_{\sigma_z Bij}^F \log_2 \lambda_{\sigma_z Bij}^F,\end{aligned}\quad (43)$$

with $\zeta = C_3^2 - 4C_3^2k + 4C_3^2k^2 - 2C_3^2p + 8C_3^2kp - 8C_3^2k^2p + C_3^2p^2 - 4C_3^2kp^2 + C_3^2k^2p^2 + 64C_1^2\Delta^2(1-k)k$ and

$$\begin{aligned}\lambda_{\sigma_z B00}^F &= \frac{1}{2}(1-k)(1 - C_3(p-1)), \\ \lambda_{\sigma_z B01}^F &= \frac{1}{2}(1-k)(1 + C_3(p-1)), \\ \lambda_{\sigma_z B10}^F &= \frac{1}{2}k(1 + C_3(p-1)), \\ \lambda_{\sigma_z B11}^F &= \frac{1}{2}k(1 + C_3 - C_3p).\end{aligned}\quad (44)$$

By tracing over A , one can obtain the reduced matrix ρ_B^F , and its eigenvalues can be given by $\lambda_{B1}^F = \frac{1}{2}(1 + C_3(2k-1)(p-1))$, $\lambda_{B2}^F = \frac{1}{2}(1 + C_3(-1 - 2k(p-1) + p))$.

Moreover, we can obtain the eigenvalues of the state $\rho_{AB}^F(t)$ are given by

$$\begin{aligned}\lambda_{AB1}^F &= \frac{1}{8}(2 - 2C_3 + 2C_3p - \sqrt{\theta}), \\ \lambda_{AB2}^F &= \frac{1}{8}(2 - 2C_3 + 2C_3p + \sqrt{\theta}), \\ \lambda_{AB3}^F &= \frac{1}{8}(2 + 2C_3 - 2C_3p - \sqrt{\theta}), \\ \lambda_{AB4}^F &= \frac{1}{8}(2 + 2C_3 - 2C_3p + \sqrt{\theta}),\end{aligned}\quad (45)$$

where $\theta = (-2 + 2C_3 - 2C_3p)^2 - 16(k - 16b^2k - 2C_3k + C_3^2k - k^2 + 16b^2k^2 + 2C_3k^2 - C_3^2k^2 + 2C_3kp - 2C_3^2kp - 2C_3k^2p + 2C_3^2k^2p + C_3^2kp^2 - C_3^2k^2p^2)$.

Explicitly, the uncertainty can be analytically given by $U^F = H(\rho_{\sigma_x B}^F) + H(\rho_{\sigma_z B}^F) + 2\sum_{k=1}^2 \lambda_{Bk}^F \log_2 \lambda_{Bk}^F$ and the bound is $U_b^F = -\sum_{i=1}^4 \lambda_{ABi}^F \log_2 \lambda_{ABi}^F$.

To illustrate how the quantum weak measurement and filtering operation steer the dynamic evolution of the uncertainty, we plot the evolution of the measuring uncertainty with the time t in the case of different operational strength s and k in figure 3. From the figure, one can obviously find that the weak measurement and the filtering operation can both

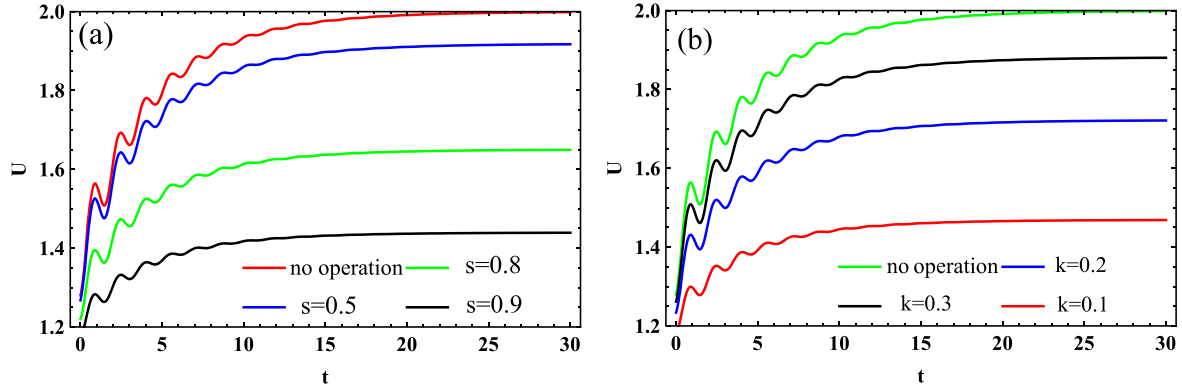


Figure 3. Uncertainty as a function of time t under DP channel for various strength, the coefficients of BDS are $C_1 = -0.5$, $C_2 = 0.4$, $C_3 = 0.8$, and we have $\gamma = 0.1$ and $\tau = 10$. Graph (a): particle A is subjected to quantum weak measurement, in this graph, the red is plotted with no operation ($s = 0$), the blue line with $s = 0.5$, the pink line with $s = 0.8$, and the black line with $s = 0.9$. Graph (b): particle A is affected by the filtering operation, in this graph, the red is plotted with the operation strength $k = 0.9$, the blue line with $k = 0.8$, the black line with $k = 0.7$, and the pink line with no operation ($k = 0.5$).

effectively reduce the magnitude of uncertainty during the incompatible measurement by adjusting the values of s and k . However, there are also differences between these two operations, when A undergoes the weak measurement, the uncertainty monotonically decreases with the growth of the parameter s , that is, the effect of reducing the uncertainty is more obvious if s is larger. The operator become identity matrix with $s = 0$. When A undergoes the filtering operation, unlike the case of weak measurement, when the value of k is closer to 0 or 1, the reduction is more effective, in fact, this operation is symmetric with $k = 0.5$. That is the result is equivalent to the case of no any operation with $k = 0.5$.

4. Applications

4.1. Entanglement witness

Quantum entanglement is deemed as one of the important manifestations of quantum correlation, and gives rise to many attractive applications in quantum information and computation, including quantum dense coding [62], quantum teleportation [64], quantum computing [65], quantum electrodynamics (QED) [66–71], and so forth. Thereby, how to conclude whether a quantum state is entangled is a basic and nontrivial task within quantum communication and computation. Herein, we briefly introduce an effective criterion based on the uncertainty relations in the current scenario. Generally speaking, $S(A|B) < 0$ is usually been considered as an indicator of entanglement witness, which shows the bound can be reduced in comparison to the equation (3) in equation (4). On the basic of equation (4), if the inequality $U = S(Q|B) + S(R|B) < \log_2 \frac{1}{c} = 1$ is true, the inequality $S(A|B) < 0$ must hold, which means the existence of entanglement between A and B .

Here we discuss the case where particle A suffers the DP channel. By setting $C_1 = C_2 = C_3 = 1$, then the initial state

has maximal purity, then calculate the entropic uncertainty, and consider $\Lambda(\nu)$ in the noise channel of B , we then can get the relationship with p and $\Lambda(\nu)$. As plotted in figure 4, one can see that the uncertainty monotonically increases with the growth of p . When $p = 0$, $U < 1$ maintains all the time and the bipartite AB is entangled, in the case of $\Lambda(\nu) \neq 0$. For $p > 0$, $U > 1$ will appear as $|\Lambda(\nu)|$ is close to 0, otherwise $U < 1$ will satisfy while $|\Lambda(\nu)|$ is far away from zero-valued. And the uncertainty will inflate with the growth of p , in this case it becomes difficult to ensure whether the system is entangled by means of the negative conditional entropy criterion. Additionally, we can also find that the value of U is symmetric with $\Lambda(\nu) = 0$ and its value is restricted by $-1 \leq \Lambda(\nu) \leq 1$. By calculating $U = 1$, we can derive its solution $\Lambda(\nu) = \pm X_m$. As a result, one can get that the relationship between X_m and p satisfies

$$2p \cdot \tanh^{-1}(1 - p) + 2 \ln \frac{2}{2 - p} - (1 + X_m(p - 1)) \ln(1 + X_m(p - 1)) - (1 - X_m(p - 1)) \ln(1 - X_m(p - 1)) = 0, \quad (46)$$

this equation is a transcendental equation, so we cannot get the exact expression of X_m , but we can calculate the numerical solution. Following the figure 4, it is easy to find X_m is the monotonically increasing function of p . In this way, we can get the range of the $\Lambda(\nu)$ when $U < 1$, is $[-1, -X_m) \cup (X_m, 1]$. That is to say, if $\Lambda(\nu)$ is in this range, we can ensure that the system is entangled in this open environment by the negative conditional entropy criterion when the maximal purity of the initial system emerges. For example, we can calculate the X_m by equation (46) and its value is $X_m = 0.678531$ with $p = 0.1$. Thereby, the entanglement condition reduces to

$$\Lambda(\nu) \in [-1, -0.678531) \cup (0.678531, 1]. \quad (47)$$

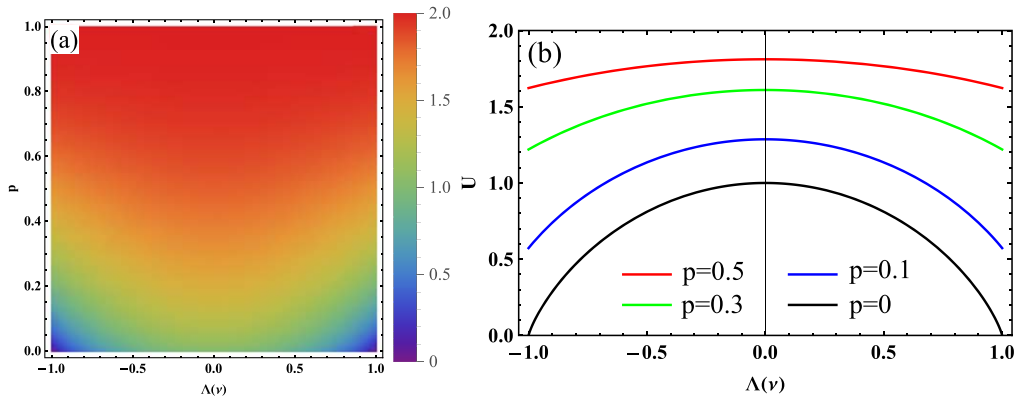


Figure 4. Evolution of entropic uncertainty U when the particle A is under DP channel. Graph (a): U as a function of the parameters $\Lambda(\nu)$ and p . Graph (b): Evolution of U with respect to $\Lambda(\nu)$ when p takes different values, the black line is plotted with $p = 0$, the blue line is plotted with $p = 0.1$, the pink line is plotted with $p = 0.3$ and the red line with $p = 0.5$. Here we set $C_1 = C_2 = C_3 = 1$.

As p becomes bigger and bigger, the range of $U < 1$ will be smaller and smaller, implying it will be more difficult to probe the systemic entanglement. In figure 4, we find that if p is greater than a threshold p_t , $U \geq 1$ will hold, which means that the method of entanglement witness will fail. To be exact, we compute the threshold p_t is 0.220056 by equation (46). More precisely, the entanglement condition ought to be

$$\Lambda(\nu) \in [-1, -X_m] \cup (X_m, 1] \quad (p < 0.220056). \quad (48)$$

With this in mind, we must keep p small if one would like to keep a composite system entangled for a long time. That is, γ should be manipulated to be small relatively, which will inhibit the affect of the DP noise on the system.

4.2. Quantum channel capacity

Typically, a quantum channel describes the situation in which any physical process acts on a quantum system [72], including transmitting secret classical information and realizing non-eavesdropping secure communication. And quantum channel capacity means the maximal amount of information transfer via quantum channel, which is described as [73]

$$C_p(\rho_{AB}) = \max\{I(\rho_{AB})\}, \quad (49)$$

where $I(\rho_{AB})$ is the mutual information of ρ_{AB} as mentioned before.

Here, we are able to build the connection between the channel capacity and the bound of the uncertainty, which can be derived as

$$U_b = \log \frac{1}{c} + S(A|B) = 1 + S(A|B), \quad (50)$$

by substituting equation (50) and the expression $I(\rho_{AB}) = S(\rho_A) + S(\rho_B) - S(\rho_{AB})$ into the equation (49), we can obtain the channel capacity $C_p(\rho_{AB})$ can be written as

$$C_p(\rho_{AB}) = \max\{S(A) - U_b + 1\}, \quad (51)$$

which shows the connection between the uncertainty relation and the quantum channel capacity.

As an illustration, we here consider this situation as before where qubit A suffers from the DP channel, with setting $C_1 = C_2 = C_3 = 1$ to make the maximal purity initial state. Thus, the reduced density matrix ρ_A is also the identity matrix $\mathbb{1}/2$, $S(\rho_A) = 1$, so we can give the exact expression of mutual information as that $I(\rho_{AB}) = 2 - U_b = \sum_{i=1}^4 \lambda_i^{AB} \log_2 \lambda_i^{AB} + 2$, which directly shows that $I(\rho_{AB})$ is linearly inversely correlated with U_b . Moreover, we offer the evolution diagram of $I(\rho_{AB})$ as a function the parameter γ and time t in figure 5 through calculating the U_b , and then obtain the $C_p(\rho_{AB})$. From the figure, we can get that $I(\rho_{AB})$ is the monotonically decreasing function of γ , that implies that the channel capacity $C_p(\rho_{AB}|\gamma, \tau) = I(\rho_{AB}|\gamma = 0, \tau)$ when the maximal purity of the initial system emerges. In this case, the eigenvalues λ_i^{AB} of ρ_{AB} are expressed as

$$\begin{aligned} \lambda_1^{AB} &= \frac{\left(1 + e^{-\frac{t}{2\tau}} \left(\cos\left(\frac{\sqrt{16\tau^2-1}t}{2\tau}\right) + \frac{\sin\left(\frac{\sqrt{16\tau^2-1}t}{2\tau}\right)}{\sqrt{16\tau^2-1}} \right) \right)}{2}, \\ \lambda_2^{AB} &= \frac{\left(1 - e^{-\frac{t}{2\tau}} \left(\cos\left(\frac{\sqrt{16\tau^2-1}t}{2\tau}\right) + \frac{\sin\left(\frac{\sqrt{16\tau^2-1}t}{2\tau}\right)}{\sqrt{16\tau^2-1}} \right) \right)}{2}, \\ \lambda_3^{AB} &= \lambda_4^{AB} = 0. \end{aligned} \quad (52)$$

In equation (52), it is easy to see that one obtains the channel capacity via eigenvalues of ρ_{AB} with a fixed τ . One can derive that the capacity is completely anti-correlated with the uncertainty, this is to say, the uncertainty can straightforward reflect the evolution of the channel capacity.

In order to show how the capacity changes in the current scenario, we plot the channel capacity as a function of the time t in terms of the equality $C_p(\rho_{AB}|\gamma, \tau) = I(\rho_{AB}|\gamma = 0, \tau)$ in figure 6. Following the figure, one can clearly find that the evolutionary trend of the capacity is oscillating periodically and reducing gradually, its amplitude remains almost a constant in a long-time limit. Here we set the stronger non-Markovian feature with $\tau = 5000$, this will lead to that the quantum channel capacity exhibits the strong oscillation. The

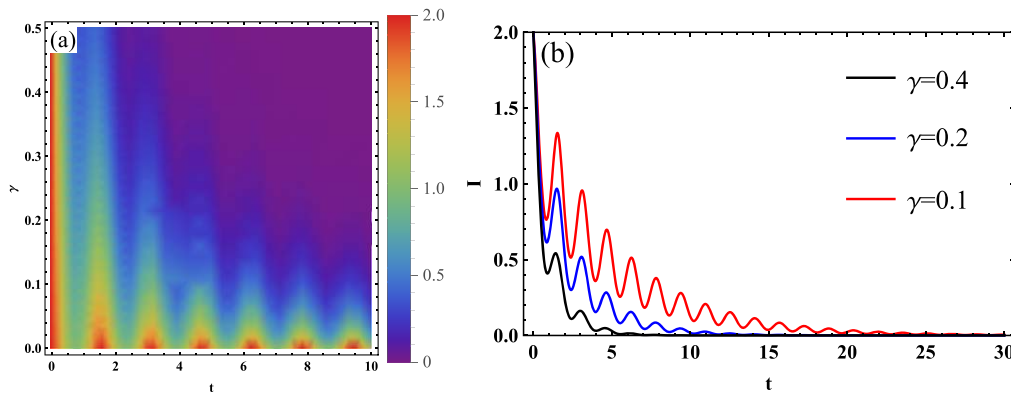


Figure 5. Evolution of mutual information I of system in DP channel, and we set $\tau = 5000$. Graph (a): mutual information I as a function of the parameter γ and time t . Graph (b): Evolution of I with respect to t when γ takes different values, the red line is plotted with $\gamma = 0.1$, the blue line is plotted with $\gamma = 0.2$ and the black line with $\gamma = 0.4$. Here we set $C_1 = C_2 = C_3 = 1$.

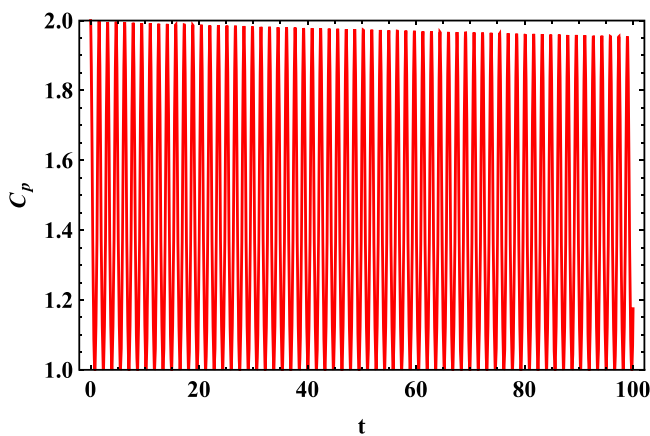


Figure 6. The quantum channel capacity C_p respected to the t for the system with $\tau = 5000$.

channel capacity could be kept in a very long time with the stronger oscillation in non-Markovian environment. Considering the above statements, due to the intrinsic relation between quantum channel capacities and the uncertainty's bound, the channel capacity can be derived analytically in the current framework.

5. Discussions and conclusions

To summarize, we have investigated the dynamics of the quantum memory-assisted entropic uncertainty in the open system where the bipartite to be probed are coupled with the environmental noises. We took into account the case that particle B suffers a colored dephasing noise and A suffers the GAD or DP channels. And we choose mutual-unbiased bases measurement of Pauli operators σ_x and σ_z as the incompatibility. It shows that the evolutionary characteristics of entropic uncertainty are obtained under the noises. We infer that the quantum memory and non-Markovian effect can essentially inhibit the increase of uncertainty and its lower bound, although the quantum correlation will be damaged

gradually by the noises. Further, we have put forward two effective operations to reduce the magnitude of the measurement's uncertainty under the open system by means of quantum weak measurement and filtering operation respectively, and compare the differences with respect to the effect of the two operations on reduction of the uncertainty. At last, we supply the applications of the QMA-EUR on entanglement witness and quantum channel capacity. Thus, we claim our investigations might be beneficial to help us understand the dynamical behavior of the entropic uncertainty in open systems and its controlling.

Acknowledgments

This work was supported by the National Science Foundation of China under Grant Nos. 61601002 and 11575001, and the fund from CAS Key Laboratory of Quantum Information under Grant No. KQI201701.

ORCID iDs

Dong Wang  <https://orcid.org/0000-0002-0545-6205>

References

- [1] Heisenberg W 1927 Über den anschaulichen Inhalt der quantentheoretischen Kinematik und Mechanik *Z. Phys.* **43** 172
- [2] Białynicki-Birula I 2007 Rényi entropy and the uncertainty relations *AIP Conf. Proc.* **889** 52
- [3] Kennard E H 1927 Zur Quantenmechanik einfacher Bewegungstypen *Z. Phys.* **44** 326
- [4] Nielsen M A and Chuang I L 2000 *Quantum Computation and Quantum Information* (Cambridge: Cambridge University Press)
- [5] Chen P F, Sun W Y, Ming F, Huang A J, Wang D and Ye L 2018 Observation of quantum-memory-assisted entropic uncertainty relation under open systems, and its steering *Laser Phys. Lett.* **15** 015206

- [6] Robertson H P 1929 The uncertainty principle *Phys. Rev.* **34** 163
- [7] Wang D, Ming F, Hu M L and Ye L 2019 Quantum-memory-assisted entropic uncertainty relations *Ann. Phys.* **531** 1900124
- [8] Deutsch D 1983 Uncertainty in quantum measurements *Phys. Rev. Lett.* **50** 631
- [9] Wehner S and Winter A 2010 Entropic uncertainty relations—a survey *New. J. Phys.* **12** 025009
- [10] Kraus K 1987 Complementary observables and uncertainty relations *Phys. Rev. D* **35** 3070
- [11] Maassen H and Uffink J B M 1988 Generalized entropic uncertainty relations *Phys. Rev. Lett.* **60** 1103
- [12] Zou H M, Fang M F, Yang B Y and Guo Y N 2014 The quantum entropic uncertainty relation and entanglement witness in the two-atom system coupling with the non-Markovian environments *Phys. Scr.* **89** 115101
- [13] Xu Z Y, Yang W L and Feng M 2012 Quantum-memory-assisted entropic uncertainty relation under noise *Phys. Rev. A* **86** 012113
- [14] Huang A J, Shi J D, Wang D and Ye L 2017 Steering quantum-memory-assisted entropic uncertainty under unital and nonunital noises via filtering operations *Quantum Inf. Process.* **16** 46
- [15] Zhang J, Zhang Y and Yu C S 2015 Entropic uncertainty relation and information exclusion relation for multiple measurements in the presence of quantum memory *Sci. Rep.* **5** 11701
- [16] Liu S, Mu L Z and Fan H 2015 Entropic uncertainty relations for multiple measurements *Phys. Rev. A* **91** 042133
- [17] Wang D, Huang A J, Hoehn R D, Ming F, Sun W Y, Shi J D, Ye L and Kais S 2017 Entropic uncertainty relations for Markovian and non-Markovian processes under a structured bosonic reservoir *Sci. Rep.* **7** 1066
- [18] Wang D, Huang A J, Sun W Y, Shi J D and Ye L 2017 Exploration of quantum-memory-assisted entropic uncertainty relations in a noninertial frame *Laser Phys. Lett.* **14** 055205
- [19] Berta M, Christandl M, Colbeck R, Renes J M and Renner R 2010 The uncertainty principle in the presence of quantum memory *Nat. Phys.* **6** 659
- [20] Kim Y H and Shih Y 1999 Experimental realization of popper’s experiment: violation of the uncertainty principle? *Found. Phys.* **29** 1849
- [21] Tomamichel M and Renner R 2011 Uncertainty relation for smooth entropies *Phys. Rev. Lett.* **106** 110506
- [22] Li C F, Xu J S, Xu X Y, Li K and Guo G C 2011 Experimental investigation of the entanglement-assisted entropic uncertainty principle *Nat. Phys.* **7** 752
- [23] Prevedel R, Hamel D R, Colbeck R, Fisher K and Resch K J 2011 Experimental investigation of the uncertainty principle in the presence of quantum memory *Nat. Phys.* **7** 757
- [24] Renes J M and Boileau J C 2009 Conjectured strong complementary information tradeoff *Phys. Rev. Lett.* **103** 020402
- [25] Coles P J, Colbeck R, Yu L and Zwolak M 2012 Uncertainty relations from simple entropic properties *Phys. Rev. Lett.* **108** 210504
- [26] Yang Y Y, Sun W Y, Shi W N, Ming F, Wang D and Ye L 2019 Dynamical characteristic of measurement uncertainty under Heisenberg spin models with Dzyaloshinskii–Moriya interactions *Frontiers Phys.* **14** 31601
- [27] Chen M N, Wang D and Ye L 2019 Characterization of dynamical measurement’s uncertainty in a two-qubit system coupled with bosonic reservoirs *Phys. Lett. A* **383** 977
- [28] Ming F, Wang D and Ye L 2019 Dynamical measurement uncertainty in the curved space-time *Ann. Phys.* **531** 1900014
- [29] Wang D, Shi W N, Hoehn R D, Ming F, Sun W Y, Kais S and Ye L 2018 Effects of hawking radiation on the entropic uncertainty in a schwarzschild space-time *Ann. Phys.* **530** 1800080
- [30] Vallone G, Marangon D G, Tamasin M and Villoresi P 2014 Quantum randomness certified by the uncertainty principle *Phys. Rev. A* **90** 052327
- [31] Certf N J, Bourennane M, Karlsson A and Gisin N 2002 Security of quantum key distribution using d-level systems *Phys. Rev. Lett.* **88** 127902
- [32] Grosshans F and Certf N J 2004 Continuous-variable quantum cryptography is secure against non-Gaussian attacks *Phys. Rev. Lett.* **92** 047905
- [33] Dupuis F, Fawzi O and Wehner S 2015 Entanglement sampling and applications *IEEE Trans. Inf. Theory* **61** 1093
- [34] König R, Wehner S and Wullschlegel J 2012 Unconditional security from noisy quantum storage *IEEE Trans. Inf. Theory* **58** 1962
- [35] Coles P J and Piani M 2014 Complementary sequential measurements generate entanglement *Phys. Rev. A* **89** 010302
- [36] Hall M J W and Wiseman H M 2012 Heisenberg-style bounds for arbitrary estimates of shift parameters including prior information *New. J. Phys.* **14** 033040
- [37] Yu C S 2017 Quantum coherence via skew information and its polygamy *Phys. Rev. A* **95** 042337
- [38] Breuer H and Petruccione F 2002 *The Theory of Open Quantum systems* (Oxford: Oxford University Press)
- [39] Daffer S, Wódkiewicz K, Cresser J D and McIver J K 2004 Depolarizing channel as a completely positive map with memory *Phys. Rev. A* **70** 010304
- [40] Karpat G, Piilo J and Maniscalco S 2015 Controlling entropic uncertainty bound through memory effects *Europhys. Lett.* **111** 50006
- [41] Wootters W K 1998 Entanglement of formation of an arbitrary state of two qubits *Phys. Rev. Lett.* **80** 2245
- [42] Chen J L, Ren C L, Chen C B, Ye X J and Pati A K 2016 Bell’s nonlocality can be detected by the violation of Einstein–Podolsky–Rosen steering inequality *Sci. Rep.* **6** 39063
- [43] Chen J L, Deng D L, Su H Y, Wu C F and Oh C H 2011 Detecting full N-particle entanglement in arbitrarily-high-dimensional systems with Bell-type inequalities *Phys. Rev. A* **83** 022316
- [44] Sun K, Ye X J, Xu J S, Xu X Y, Tang J S, Wu Y C, Chen J L, Li C F and Guo G C 2016 Experimental quantification of asymmetric Einstein–Podolsky–Rosen steering *Phys. Rev. Lett.* **116** 160404
- [45] Wang J C, Cao H X, Jing J L and Fan H 2016 Gaussian quantum steering and its asymmetry in curved spacetime *Phys. Rev. D* **93** 125011
- [46] He Q Y and Reid M D 2013 Genuine multipartite Einstein–Podolsky–Rosen steering *Phys. Rev. Lett.* **111** 250403
- [47] Ollivier H and Zurek W H 2001 Quantum discord: a measure of the quantumness of correlations *Phys. Rev. Lett.* **88** 017901
- [48] Wang D, Huang A J, Ming F, Sun W Y, Lu H P, Liu C C and Ye L 2017 Quantum-memory-assisted entropic uncertainty relation in a Heisenberg XYZ chain with an inhomogeneous magnetic field *Laser Phys. Lett.* **14** 065203
- [49] Hu M L, Hu X Y, Peng Y, Zhang Y R and Fan H 2018 Quantum coherence and geometric quantum discord *Phys. Rep.* **762–4** 1
- [50] Xu J S, Sun K, Li C F, Xu X Y, Guo G C, Andersson E, Franco R L and Compagno G 2013 Experimental recovery of quantum correlations in absence of system-environment back-action *Nat. Commun.* **4** 2851

- [51] Xu J S, Xu X Y, Li C F, Zhang C J, Zou X B and Guo G C 2010 Experimental investigation of classical and quantum correlations under decoherence *Nat. Commun.* **1** 7
- [52] Li C F, Xu J S, Xu X Y, Li K and Guo G C 2011 Experimental investigation of the entanglement-assisted entropic uncertainty principle *Nat. Phys.* **7** 752
- [53] Ding Z Y, Yang H, Yuan H, Wang D, Yang J and Ye L 2019 Experimental investigation of nonlocal advantage of quantum coherence *Phys. Rev. A* **100** 022308
- [54] Aharonov Y, Albert D Z and Vaidman L 1988 How the result of a measurement of a component of the spin of a spin-1/2 particle can turn out to be 100 *Phys. Rev. Lett.* **60** 1351
- [55] Wang S C, Yu Z W, Zou W J and Wang X B 2014 Protecting quantum states from decoherence of finite temperature using weak measurement *Phys. Rev. A* **89** 022318
- [56] Xiao X and Li Y L 2013 Protecting qutrit-qutrit entanglement by weak measurement and reversal *Eur. Phys. J. D* **67** 204
- [57] Gisin N 1996 Hidden quantum non-locality revealed by local filters *Phys. Lett. A* **210** 151
- [58] Hirsch F, Quintino M T, Bowles J and Brunner N 2013 Genuine hidden quantum nonlocality *Phys. Rev. Lett.* **111** 160402
- [59] Sun Q, Al-Amri M, Davidovich L and Zubairy M S 2010 Reversing entanglement change by a weak measurement *Phys. Rev. A* **82** 052323
- [60] Siomau M and Kamli A A 2012 Defeating entanglement sudden death by a single local filtering *Phys. Rev. A* **86** 032304
- [61] Karmakar S, Sen A, Bhar A and Sarkar D 2015 Effect of local filtering on freezing phenomena of quantum correlation *Quantum Inf. Process.* **14** 2517
- [62] Bennett C H and Wiesner S J 1992 Communication via one- and two-particle operators on Einstein–Podolsky–Rosen states *Phys. Rev. Lett.* **69** 2881
- [63] Murao M, Jonathan D, Plenio M B and Vedral V 1999 Quantum telecloning and multiparticle entanglement *Phys. Rev. A* **59** 156
- [64] Bennett C H, Brassard G, Crépeau C, Jozsa R, Peres A and Wootters W K 1993 Teleporting an unknown quantum state via dual classical and Einstein–Podolsky–Rosen channels *Phys. Rev. Lett.* **70** 1895
- [65] Kok P, Munro W J, Nemoto K, Ralph T C, Dowling J P and Milburn G J 2007 Linear optical quantum computing with photonic qubits *Rev. Mod. Phys.* **79** 135
- [66] Mirza I M and Schotland J C 2016 Multiqubit entanglement in bidirectional-chiral-waveguide QED *Phys. Rev. A* **94** 012302
- [67] Armata F, Calajo G, Jaako T, Kim M S and Rabl P 2017 Harvesting multiqubit entanglement from ultrastrong interactions in circuit quantum electrodynamics *Phys. Rev. Lett.* **119** 183602
- [68] Mirza I M and Schotland J C 2016 Two-photon entanglement in multiqubit bidirectional-waveguide QED *Phys. Rev. A* **94** 012309
- [69] Gheeraert N, Zhang X H H, Sépulcre T, Bera S, Roch N, Baranger H U and Florens S 2018 Particle production in ultra-strong coupling waveguide QED *Phys. Rev. A* **98** 043816
- [70] Mirza I M 2015 Bi- and uni-photon entanglement in two-way cascaded fiber-coupled atom-cavity systems *Phys. Lett. A* **379** 1643
- [71] Gu X, Kockum A F, Miranowicz A, Liu Y and Nori F 2017 Microwave photonics with superconducting quantum circuits *Phys. Rep.* **718–9** 1
- [72] Lim Y and Lee S 2018 Activation of the quantum capacity of Gaussian channels *Phys. Rev. A* **98** 012326
- [73] Li C Z, Huang M Q, Chen P X and Liang L M 2000 *Quantum Communication and Quantum Computing* (Changsha: National University of Defense Technology Press)